A Multi-Metrics Optimization Model for Non-rigid Registration Using Free-Form Deformation

Jiasi Song[1], Lixu Gu*[1], Pengfei Huang[1], Wei Li[1] and Jianrong Xu*[2]

[1] Image-Guided Surgery Laboratory, Shanghai Jiao Tong University, 800 Dongchuan Rd, Shanghai, 200240 China

[2] Renji Hospital of Medical School, Shanghai Jiao Tong University, China

ABSTRACT

We propose a new optimization model for non-rigid registration of images using multi-metrics. The ordinary searching step of optimization has been often trapped in local minima and produces wrong registration results. In this paper, if the condition occurs, multi-metrics model will switch to the other metrics to get rid of the local minima, vice versa, until optimization cannot proceed any more for any of the metrics. We have tested our approach in a variety of experimental conditions and compared the results with the optimization without multi-metrics. The results indicate that the new model is robust and fast in non-rigid registration.

Keywords: Multi-Metrics, Registration, Free-Form Deformation, Optimization

1. INTRODUCTION

Given two image sets acquired from the same patient but at different time or by different devices, image registration is the process of finding a geometric transformation between the two respective image-based coordinate systems that maps a point in the first image set to the point in the second set that has the same patient-based coordinates, i.e. represents the same anatomic location [1]. This notion presupposes that the anatomy is the same in the two image sets, an assumption that may not be precisely true if, for example, the patient has had a surgical resection between the two acquisitions [2].

Non-rigid image registration is an increasingly important technology in both clinical and research applications [11]. And it has been demonstrated by Mattes et al. [1] that the Free-Form Deformation is a feasible approach, capable of accurate non-rigid registrations.

However, current popular metrics such as mean squares metric [3], [5], mutual information metric [7], [8] and normal vector information [4] all have several local minima in the high dimension of the parameter vector μ of FFD [5], [6], [12]. Also various optimization strategies, like steepest gradient-descent method [4], [5], and BFGS method [6] are easy being trapped in these local minima, which will lead to a wrong result of registration. Those make the minimization process a difficult optimization problem.

This work focuses on optimization using more than one metric, that is, using metrics alternatively, switch the registration metric from one to another when the optimization process finds a result. This will avoid the searching step of optimization from trapping in local minima to a large extent.

The paper is organized as follow: In Section 2, we gave the criterion of metrics and Free-Form Deformation, and Section 3 is the optimization process using multi-metrics. Section 4 describes the results of the experiments, and conclusions are given in Section 5.

2. METHODS

2.1 Free-Form Deformation

* Corresponding authors: Jianrong Xu and Lixu Gu (e-mail gu-lx@cs.sjtu.edu.cn; phone 8621-34204137; fax 8621-34204145; http://se.sjtu.edu.cn/igst)

The FFD model is based on B-splines [1], [9]. The basic idea of FFD is to deform an object by manipulating an underlying mesh of control points. The resulting deformation controls the shape of the 3-D or 2-D object and produces a smooth and C^2 continuous transformation.

To define a spline-based FFD, we denote the domain of the image volume as $\Omega = \{(x, y, z) \mid 0 \le x < X, 0 \le y < Y, 0 \le z < Z\}$ [1]. Let Φ denote a $n_x \times n_y \times n_z$ mesh of control points $\phi_{i,j,k}$ (μ_l) with uniform spacing δ. Then, the FFD can be written as the 3-D tensor product of the familiar 1-D cubic B-splines:

$$T_{local}(x, y, z) = \sum_{l=0}^{3} \sum_{m=0}^{3} \sum_{n=0}^{3} B_l(u) B_m(v) B_n(w) \phi_{i+l, j+m, k+n} \tag{1}$$

where $i = \lfloor x / n_x \rfloor - 1$, $j = \lfloor y / n_y \rfloor - 1$, $k = \lfloor z / n_z \rfloor - 1$, $u = x / n_x - \lfloor x / n_x \rfloor$, $v = y / n_y - \lfloor y / n_y \rfloor$, $w = z / n_z - \lfloor z / n_z \rfloor$ and where B_l represents the l th basis function of the B-spline

$$\begin{aligned} B_0(u) &= (1-u)^3 / 6 \\ B_1(u) &= (3u^3 - 6u^2 + 4) / 6 \\ B_2(u) &= (-3u^3 + 3u^2 + 3u + 1) / 6 \\ B_3(u) &= u^3 / 6 \end{aligned} \tag{2}$$

2.2 Mutual Information

The mutual information of two images is based on the concept of information theory and expresses the amount of information that one image A contains about a second image B [8], which is a combination of the entropy values of the images, both separately and jointly.

Entropy can be interpreted as a measure of dispersion of a probability distribution. It is low when a distribution has a few sharply defined, dominant peaks and it is maximal when the distribution is uniform.

Here, we use Mattes et al. [1] implementation for the MI computation. The negative of mutual information S between the reference image and the transformed test image as the measure can be expressed as a function of the transformation parameters μ:

$$S(\mu) = -\sum_{\iota} \sum_{\kappa} p(\iota, \kappa \mid \mu) \log \frac{p(\iota, \kappa \mid \mu)}{p_T(\iota \mid \mu) p_R(\kappa)} \tag{3}$$

Where p, p_T and p_R are the joint, marginal test, and marginal reference probability distributions, respectively. The histogram bins are indexed by integer values $\kappa, 0 \le \kappa \le L_R$ and $\iota, 0 \le \iota \le L_T$, where L_R and L_T are specified numbers of uniformly sized bin along the respective dimensions of the joint histogram of the reference and test images.

2.3 Normal Vector Based Similarity Measure

We propose a new metric computed from the normal vector (NV) instead of cultural method using pixel grey value. The NV of a point in an image is the NV of a contour line for two-dimensional (2D) images or the NV of an iso-surface for three-dimensional (3D) images, basing the contour or iso-surface on the gray level of the point.

In the NV based measure, the difference between the NVs in the test and reference images is summed to evaluate the similarity between these two images, which is similar to the mean squared intensity difference measure that computes the intensity difference between pixels in the test image and pixels in the reference image to assess the similarity between them. As the cosine value of the included angle of two vectors can be adopted to evaluate the difference between them, the mean of the squared cosine included angle of the corresponding NV values in the two images can be used to evaluate how closely the two images are registered.

Let T be the test image when registered to the reference image R by applying the transformation F. The NV based

measure S is employed as the similarity criterion in our registration framework, and defined as:

$$S(T,R,F)=\frac{1}{card(V)}\sum_{X\in V}\cos^2\theta(N_T(X),N_R(F(X))) \tag{4}$$

Where, card(V) is the size of the volume(V) that the measure samples points within the test image T; X is the coordinate of point P from V; F(X) means the coordinate of P' in the reference image mapped from P in image T by transformation F. $N_T(X)$ denotes the transformed NV value of point P; $N_R(F(X))$ is the NV of the corresponding point P' in transformed image R. θ represents the included angle between the two NV vectors.

2.4 Mean Squares Metric

Mean squares metric computes the mean squared pixel-wise difference in intensity between the test image T and the reference image R over a user defined region:

$$MS(T,R)=\frac{1}{N}\sum_{i=1}^{N}(T_i-R_i)^2 \tag{5}$$

Where, T_i is the i-th pixel of Image T, R_i is the i-th pixel of Image R, N is the number of pixels considered.

The optimal value of the metric is zero. Poor matches between images T and R result in large values of the metric. This metric is simple to compute and has a relatively large capture radius. It relies on the assumption that intensity representing the same homologous point must be the same in both images. Hence, its use is restricted to images of the same modality. Additionally, any linear changes in the intensity result in a poor match value.

3. MULTI-METRICS OPTIMIZATION METHOD

To find the optimal transformation, we improve the L-BFGS-B optimization (Broyden- Fletcher- Goldfarb- Shanno) [5], [6], [10], a limited-memory, quasi-Newton minimization package, to reduce the cost function until termination criterion is satisfied. The limited-memory method is useful here because of the high dimensionality of the parameter space. Instead of estimating the entire Hessian during minimization, only a low-rank approximation is calculated, allowing linear or super-linear convergence rates.

The advantage of the L-BFGS-B method is the speed that it can reach the minima quickly. However, the method can not avoid the searching step from being trapped in local minima. In the other side, the robustness of the measures is questionable. Hence we propose a hybrid optimization model based on multi-metrics for the reason that there is much less chance for a point in the searching space being trapped at the local minima of various metrics at the same time than of single metric.

The optimization is stated as a function:

$$\hat{\mu}=\arg\min(-M^{\mu_0,F}(\mu)) \tag{6}$$

Where $M^{\mu_0,F}(\mu)$ denotes the similarity measure as a function of the parameters, the B-spline coefficients μ. μ_0 denotes the initial coefficients of optimization, and F is the termination criterion, the function for judging whether to terminate the optimization process.

First set one of the metrics M_1 as M, and its corresponding terminating function F_1 as F, then search the minimum. After the L-BFGS-B optimization process stopped, which means $\hat{\mu}$ may have been found, change M for the other metric M_2, set the resulted $\hat{\mu}$ as μ_0 and F_2 as F, start the optimization again, which can be demonstrated as:

$$\hat{\mu}=\arg\min(-M_2^{\arg\min(-M_1^{\mu_0,F_1}(\mu)),F_2}(\mu)) \tag{7}$$

When find another minimum, switch back the metric and start optimization again. Repeat the above procession, until the

Initialize μ_0
Repeat
    Set M_1 as the measure M
    Set F_1 as F
  Do L-BFGS-B to calculate $\arg\min(-M^{\mu_0,F}(\mu))$
  Set the optimization result above as μ_0
  Set M_2 as the measure M
    Set F_2 as F
  Do L-BFGS-B to calculate $\arg\min(-M^{\mu_0,F}(\mu))$
  Set the optimization result above as μ_0
Until both of the optimization processes can not proceeds any more

Figure 1: The optimization algorithm based on multi-metrics

optimization cannot proceed any more for both of the metrics, which equals that the value of μ_i is the same as μ_{i-1} and μ_{i-2}, then μ_i is the found global minima.

The hybrid optimization process is shown in Fig.1.

4. EXPERIMENTS

In the following, examples based on the proposed approach for MRI-MRI and CT-MRI registration tasks are presented. The results of each registration are given to evaluate the performance. The programs are based on MS Visual C++ environment and run on a P-IV 2.60 GHz PC with 512MB main memory and MS Windows XP.

In the registration, we adopt linear interpolation when needed and use improved L-BFGS-B optimization.

In fact, the L-BFGS-B method needs the derivatives of the metric with respect to the parameters μ. However, different metrics cost different time for calculating derivatives, e.g. the Mattes implementation of Mutual information is much faster than Mean Squares Metric or NVI, for the reason it cost less time in calculating derivatives. In order to accelerate the minimization process, we adjust the optimization model, altering the parameters of BFGS optimization for the slower metric to reduce the iteration number of searching.

4.1 MRI-MRI Registration

In the Mono-Modality experiments, both MI and Mean Squares Metric (MS) are used in the registration (calculating NVI and its derivatives cost much more time than them), and two groups of experiments on 2D MRI images of the brain are performed. In these experiments, the B-spline deformations all used 10×10 control mesh.

In the first experiment, the images for non-rigid registration are shown in Fig.2 (a) and (b). Both images are of size 256×256. As Fig.2 shows, (c) is the difference image between (a) and (b), (d)- (f) are the transformed test image after registration using MI, MS, MI & MS, respectively, (g)-(i) are the difference images after the three methods of registration. Correspondingly, Table.1 shows the registration time, Squared Sum of Intensity Difference (SSD) and Correlation Coefficient (CC) of them.

It is clear that the registration using MI only is the fastest method of the three that only need 5.016s to finish registration, but the result is unsatisfactory for the reason that MI metric has trapped the searching process in local minima. On the other hand, the registration using only MS demonstrates a good result of image alignment, but costs too much time for calculating. The Multi-metrics model integrates the advantages of the two methods above, it cost less time and produce a satisfactory registration result.

Next, we still used the Fig.1 (a) as the test image, and transformed it by 5 groups of randomized parameters, then add 1% noise randomly in the transformed images. The noised images are performed registration with Fig 1(a), and in these experiments, the maximum number of optimizing iteration for MS metric in Multi-metrics model is set to 5 in order to reduce the cost time for registration.

Table 1: Registration time, SSD and CC of optimization using MI, MS, MI&MS, respectively.

	Before Registration	MI	MS	MI&MS
Run time	—	5.016s	403.157s	320.797s
SSD(mean)	2073.86	429.056	2.502	2.511
CC	0.85809	0．96089	0．97976	0．98089

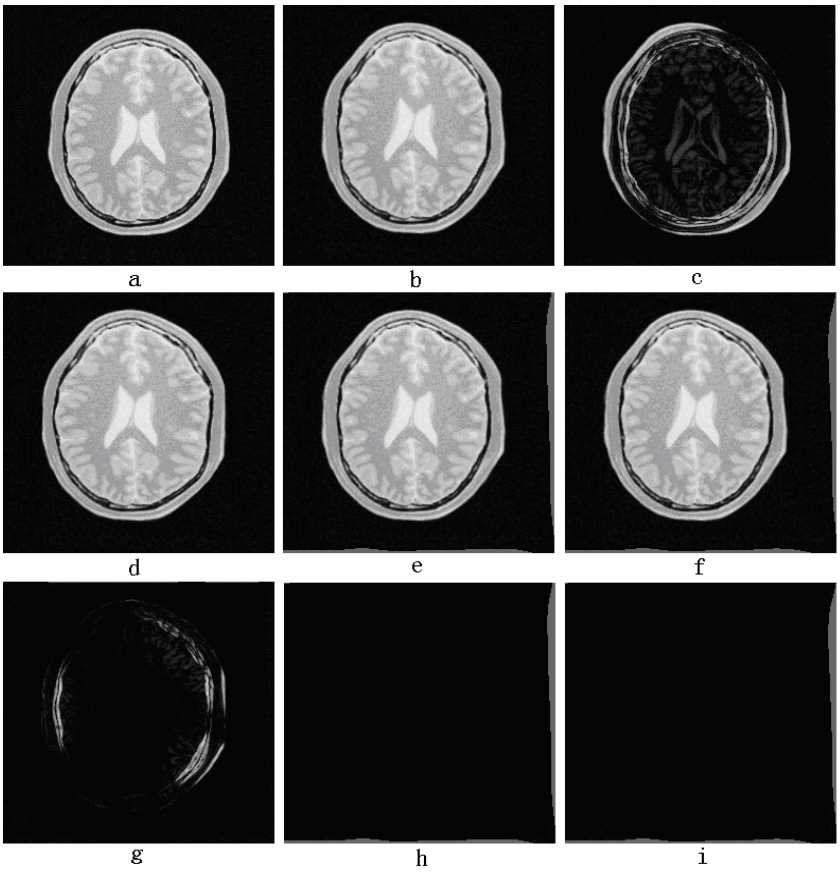

Figure 2: Registration images: (a) The test image; (b) The reference image; (c) the difference image between (a) and (b); (d)-(f) the transformed test image after registration using MI only; Mean Squares Metric only; MI & Mean Squares Metric for multi-metrics optimization model, respectively; (g)-(i) the difference image between image (d)-(f) and (b), respectively.

Table 2 : Registration time, SSD and CC of optimization using MI, MS, MI&MS, respectively.

	MI			MS			MI&MS		
	Time(s)	SSD	CC	Time(s)	SSD	CC	Time(s)	SSD	CC
Data1	7.156	392.41	0.97323	163.745	227.068	0.97856	33.703	225.484	0.97922
Data2	2.359	400.13	0.93154	77.843	229.13	0.97328	29.5	230.085	0.97790
Data3	5.297	433.98	0.95659	83.312	233.464	0.97695	44.015	231.029	0.97639
Data4	4.875	423.01	0.94493	77.765	249.693	0.97721	43.312	249.67	0.97545
Data5	10.218	305.08	0.97006	63.531	238.311	0.97424	32.531	238.82	0.9766

The registration results are demonstrated in Table.2, and Fig.3 presents the searching route of three optimization methods for data1 (the 1st row in Table.2), which shows that the MI&MS optimization is still robust with 1% noise while the MI optimization route stops at a higher SSD value than it, and the speed of optimization using MI&MS is almost 2 times of the method using MS only.

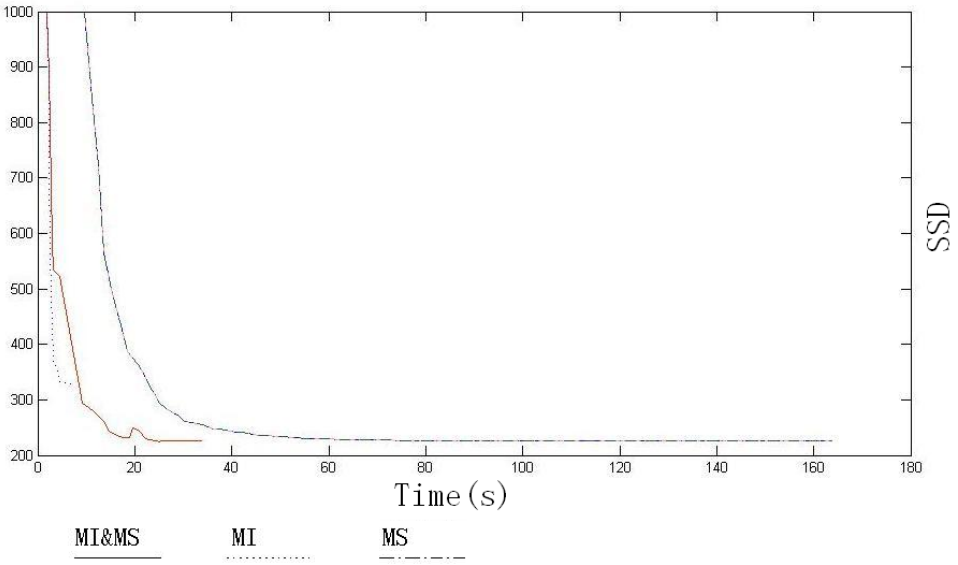

Figure 3: The searching routes of optimization using MI&MS, optimization using MI only and optimization using MS only.

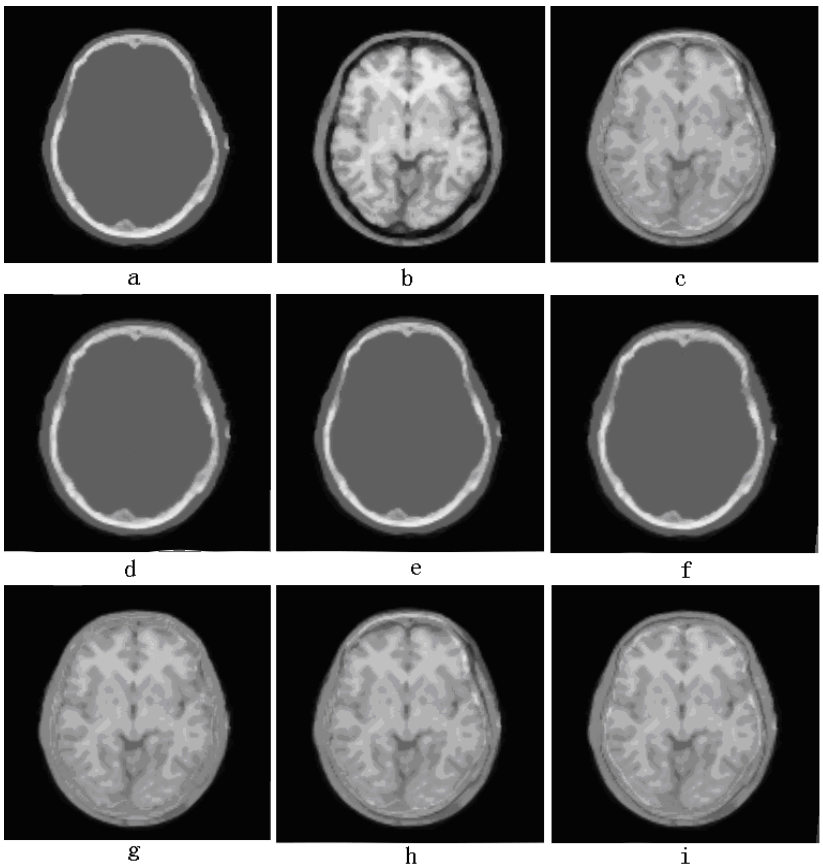

Figure 4: Registration images: (a) The test image; (b) The reference image; (c)-(e) the transformed test image after registration using MI only; NVI only; MI & NVI for multi-metrics optimization model, respectively; (f)-(h) the fusion image between image (c)-(e) and (b), respectively.

4.2 CT-MRI Registration

In multi-modality registration, because MS can only be used for mono-modality, Normal Vector Information metric (NVI) and MI are used to do registration. The 2D images being registered are both of size 250×250. In these experiments, the B-spline deformations are used 6×6, 10×10, 14×14 control mesh, respectively.

Fig. 4 shows the registration result of 14×14 control mesh. Fig.4 (a) is the test image, (b) is the reference image; (c)-(e) are transformed test image after registration using MI, NVI, MI &NVI, respectively, (f)-(h) are the fusion images after the three methods of registration. Moreover, Table.3 shows the registration time and final MI values of registration using 6×6, 10×10, 14×14 control mesh.

Table 3: Registration time and MI of optimization using MI, NVI, MI&NVI, for control mesh14*14, 10*10, 6*6 respectively.

	MI	NVI	MI&NVI
Run time(s) (14*14)	4.281	3598.47	621.047
MI (14*14)	0.93987	0.86852	0.96109
Run time (s)(10*10)	5.797	2391.05	496.641
MI (10*10)	0.93779	0.87203	0.97389
Run time (s)(6*6)	2.047	2213.5	271.045
MI (6*6)	0.89396	0.85343	0.93515

The table demonstrated that in multi-modality registration, optimization method using MI only is still fast but easy being trapped in local minima. NVI metric and its gradient need much more time to calculate than MI, and produce worse result. The multi-metrics optimization model produces the most accurate registration result in three, and its registration process does not need so much time as NVI does.

5. CONCLUSION

In this paper, we present a novel multi-metrics optimization model for non-rigid registration using FFD. It is tested feasible. Compared to the optimization using only one metric, the model is more robust. If one of the chosen metric for multi-metrics model costs much time for computing value and gradients, adjusting the optimization parameters for this metric can accelerate the optimization process.

The initial framework is proposed here and we will pay more efforts to exploit its further merits. As the further work, we are scheduling to find another multi-modality metric which is faster than NVI to cooperate with MI to do multi-modality registration.

6. ACKNOWLEDGEMENT

The authors would like to thank the doctors from Shanghai Renji hospital in providing the experiment data and clinical advices. We are also grateful for the intellectual and financial support of National Natural Science Foundation (60571061), 863 research foundation (2007AA01Z312), and the Shanghai municipal research foundation (06dz15010).

REFERENCES

1. D. Mattes, D. R. Haynor, H. Vesselle, T. K. Lewellen, and W. Eubank, “PET-CT image registration in the chest using free-form deformations,” IEEE Transactions on Medical Imaging 22(1), pp. 120–128, 2003
2. Frank. Sauer, “Application Image Registration: Enabling Technology for Image Guided Surgery and Therapy,”

3. G. P. Penney, J. Weese, J. A. Little, P. Desmedt, D. L.G. Hill, D. J. Hawkes, “A comparison of similarity measures for use in 2D-3D medical image registration,” IEEE Transactions on Medical Imaging, vol. 17, no. 4, pp.586-595, 1999
4. Xiahai Zhuang, Lixu Gu, and Jianfeng Xu, “Medical Image Alignment by Normal Vector Information,” Y. Hao et al. (Eds.): CIS 2005, Part I, LNAI 3801, pp. 890 – 895, Springer-Verlag Berlin Heidelberg, 2005
5. J. W. Pluim, J. B. Antoine Maintz, and M.A. Viergever, “Mutual-Information-Based Registration of Medical Images: A Survey,” IEEE Transactions On Medical Imaging, Vol. 22, No. 8, August 2003
6. P.Thevenaz and M. Unser, “Optimization of mutual information for multiresolution image registration,” IEEE Transactions on Image Processing 9(12), pp. 2083-2099 2000
7. J P.W. Pluim, J. B. A. Maintz, and M.A. Viergever, “Image Registration by maximization of combined mutual information and gradient information,” IEEE Transaction On Medical Imaging, 19(8) 2000
8. P. Viola and W. M. Wells III, “Alignment by maximization of mutual information,” in Proc. 5th Int. Conf. Computer Vision, Boston, MA, June 20–23, 1995, pp. 16–23.
9. S. Y. Lee, K. Y. Chwa, S. Y. Shin, “Image Metamorphosis Using Snakes and Free-Form Deformations”, In Computer Graphics (Proc.SIGGRAPH), 1995, pp. 439-448.
10. L. Ibanez, W. Schroeder, L. Ng, J. Cates. “The ITK Software Guide,” Insight Software Consortium, August 2003.
11. L. Ng, “Overview: ITK Registration Methods,” SPIE2004: Medical Image Segmentation and Registration with ITK, 2004.
12. S. Klein*, M. Staring, and J. P.W. Pluim, “Comparison of gradient approximation technicques for optimization of mutual information in nonrigid registration,” Medical Imaging 2005: Image Processing, Proc. Of SPIE Vol 5747